

Evidence of Partial Draining for Linear Polyelectrolytes: Heparin, Chondroitin 6-Sulfate, and Poly(styrenesulfonate)

Robert M. Peitzsch, Martha J. Burt, and Wayne F. Reed*

Department of Physics, Tulane University, New Orleans, Louisiana 70118

Received April 29, 1991; Revised Manuscript Received October 16, 1991

ABSTRACT: Zero polymer concentration diffusion coefficients, D_0 , of heparin and chondroitin 6-sulfate were independent of ionic strength C_s . Since static dimensions of such linear polyelectrolytes are sensitive functions of C_s , the constant D_0 may represent a partial-draining effect. Similar measurements were made for poly(styrenesulfonate) fractions. For high molecular weights root-mean-square (RMS) radii of gyration $\langle S^2 \rangle^{1/2}$ vs C_s were determined. $1/D_0$ followed $\langle S^2 \rangle^{1/2}$ at high C_s (>100 mM), climbed less steeply at intermediate C_s , and reached a plateau below 30 mM. Although tempting to interpret these regimes as nondraining, partial draining, and free draining, respectively, $1/D_0 \propto M^{0.5}$ for all C_s . Thus, although some type of draining condition seems implicated, a simplistic free-draining condition in the plateau region is inconsistent with the mass scaling. The data show that dynamic light scattering may not be an appropriate particle sizing technique for many linear polyelectrolytes. The "extraordinary" diffusional phase, present in some samples, could always be permanently removed by filtration through membranes of sufficiently small pore size.

Introduction

The hydrodynamic behavior of macromolecules depends on such factors as linear dimensions, excluded volume, and degree of draining. Numerous theoretical approaches have been taken for calculating such quantities as intrinsic viscosity, sedimentation coefficients, and translational and rotational friction factors.¹⁻⁸ It is not the object of this report to make critical comparisons of the theories but rather to provide data which bear directly on one of the fundamental issues necessarily addressed in theories of the translational diffusion coefficient: the relationship between the polymer's root-mean-square (RMS) radius of gyration $\langle S^2 \rangle^{1/2}$ and the frictional coefficient f .

The so-called Staudinger law required proportionality between intrinsic viscosity, $[\eta]$, and molecular weight, M ; i.e., it required free draining of the polymer. Hydrodynamically, free draining implies that the perturbation to the solvent flow field caused by one resistive unit of a polymer chain has no effect on the flow fields near other units. The Staudinger law was seen to break down for larger polymers, for which $[\eta]$ could increase as a weaker power of M . Debye⁹ proposed a hydrodynamic screening effect, whereby the peripheral units of the polymer would partially screen more interior units from the solvent flow. The limiting case of strong screening is often called the "nondraining" condition. In this limit, for the case of no excluded volume (θ solvent), $[\eta]$ and the friction factor f vary as $M^{0.5}$. In the nondraining limit these quantities are measures of the polymer's linear dimension, just as in the case of, say, impermeable spheres. Recently, Mulderje and Jalink¹⁰ calculated that there is always appreciable differential flow of solvent between the polymer center of mass and the outer coil segments, so that the term "least-draining limit" may be more appropriate than "nondraining limit".

While the free-draining and nondraining limits yield fairly well agreed upon forms for the hydrodynamic coefficients of random coils and wormlike chains, the intermediate regime of partial draining becomes more critically dependent on the types of physical and mathematical approximations made. Perhaps because of this complexity, and perhaps even more so because of the non-draining nature of the data for polymers in near θ

conditions in organic solvents, it has been widely assumed that real coil polymers generally behave as nondraining entities. There are a number of implications to this latter assumption, among them the notion that measurement of diffusion coefficients via dynamic light scattering, for example, is linearly related to the polymer's linear dimension, e.g., to the root-mean-square radius of gyration. Thus, dynamic light scattering is a widely used polymer sizing technique, although, as the current data will show, it must be used cautiously for polyelectrolyte sizing when f ceases to be proportional to $\langle S^2 \rangle^{1/2}$. The implications of draining for biological polymers, which exist in a solvent milieu rich in varied ionic species, are less clear but probably quite important. The hydraulic permeability and kinetics of deformation of connective tissues under load, cartilage, for example, may be closely related to draining properties.

This work presents evidence for the independence of the diffusion coefficient extrapolated to zero polymer concentration, D_0 , from the ionic strength, C_s (expressed in millimolar throughout) and hence from $\langle S^2 \rangle^{1/2}$ for two biological polyelectrolytes, heparin (Hep) and chondroitin 6-sulfate (ChS). Glycosaminoglycans (GAG) such as ChS play a structural role, being found either as individual molecules in the ground and connective tissues of the body or as parts of large aggregates (proteoglycans) in cartilage.¹¹ Heparin, on the other hand, while also a GAG, plays the role of an anticoagulant and is generally found in mast cells along with serotonin and other parts of the body's "first-aid kit".

Previous studies on another GAG, hyaluronate¹² (HA), as well as on a variably ionized, long synthetic polyelectrolyte, copolymers of polyacrylamide/polyacrylate (NaPAA),¹³ also showed D_0 , extrapolated to zero scattering angle θ , as well as to zero polymer concentration, to be independent of C_s . In those cases a large, measurable expansion of mean-square radius of gyration $\langle S^2 \rangle$ occurred as C_s was reduced over the range of roughly 1 M to 1 mM, thus showing the independence of D_0 from static dimensions. The extrapolation of D_0 to $\theta = 0^\circ$ eliminated the possible contribution to D_0 of internal flexional modes of individual polymers at nonzero θ . In those works, respectively, it was found that for HA $\langle S^2 \rangle = M(87 + 307/C_s^{0.5})/120$ and that for NaPAA $\langle S^2 \rangle = M(27 + 350/C_s^{0.5})/86$. In these expressions $\langle S^2 \rangle$ is in angstroms squared, M

* To whom correspondence should be addressed.

is the polymer molecular weight, and in the latter ξ is the Manning parameter for the variably ionized NaPAA. Unfortunately, heparin and chondroitin 6-sulfate are too small for their $\langle S^2 \rangle$ to be measurable with visible light, so their change in static dimension with C_s must be inferred on the basis of the general phenomenon seen for a wide range of linear polyelectrolytes.

In fact, advantage is taken of fairly monodisperse fractions of a sulfated linear polyelectrolyte, poly(styrene-sulfonate) (NaPSS), to explore the validity of the partial-draining conclusion by trying to follow the transition from nondraining to presumably partial draining as the ionic strength C_s of the solution is decreased. This is accomplished by making radius of gyration measurements as a function of C_s in addition to extrapolating diffusion coefficients to zero polymer concentration C_p , at different values of C_s . As has been long suspected on intuitive grounds, the stiffer and hence more "open" the structure of a polymer, the more freely the solvent might be expected to drain through it. Since flexible polyelectrolytes can undergo large changes in dimension as the ionic strength changes, it is not surprising that the degree of draining might also change. What would appear to be clear evidence of transitions from nondraining at high C_s , to partial draining at intermediate C_s (30–100 mM), to free draining below about 30 mM C_s , however, is confounded by the dependence of f on $M^{0.5}$ in the three regimes.

Materials and Methods

Materials. Triton-free mixed ester cellulose filters with a pore size of 0.22 μm were obtained from Millipore (Millex-GS series). Metrical polypropylene filters with a pore size of 0.1 μm were obtained from Gellman Sciences. Durapore (PVDF) filters with a pore size of 0.1 μm were obtained from Millipore (Millex-VV series). Mixed esters of cellulose filters with a pore size of 0.05 μm were obtained from Millipore (MF series). With the exception of the 0.1- μm filters from Gellman Sciences, the filters were hydrophilic and were flushed with 10–20 mL of distilled deionized H_2O before use. The Gellman Science's filters were hydrophobic and were wetted with methanol before being flushed with distilled deionized H_2O . No difference in the data was obtained using either of the 0.1- μm filters.

All samples were prepared in deionized, distilled, 0.22- μm -filtered H_2O , whose conductivity was less than 1 μS .

Heparin, extracted from porcine intestinal mucosa, was obtained from SchweitzerHall (Lot Nos. 145471, 146367, and 147242) and used as supplied. Heparin from other suppliers (Calbiochem, ICN, Polysciences, Sigma, and USBiochemicals) was also tested. However, upon being checked for the presence of an "extraordinary phase", EP (i.e., a phase for which an anomalously low diffusion coefficient is measured at low C_s , which quickly gives way to a higher, classically explainable D at a certain, usually low value of C_s),¹⁴ it was found that only the SchweitzerHall and USBiochemicals samples were without this phase. There is evidence that this phase may represent a small population of aggregates of polyelectrolyte chains or perhaps entanglements. In all cases, this "extraordinary" phase could be permanently removed by filtration through a filter membrane of sufficiently small pore size. A 0.1- μm filter was sufficient to remove this phase in most of the samples. The ICN sample, however, which had a very strong signal before filtering, required a 0.05- μm filter to remove the EP. If these samples were filtered through 0.22- μm or larger pore size membranes, then the EP persisted. In addition, by qualitative observation through a microscope, there was a correlation between the degree of crystallinity of the dry sample and the lack of the extraordinary phase. Those without this phase appeared to be the most crystalline.¹⁵

Chondroitin 6-sulfate, extracted from shark cartilage, was obtained from Pfaltz-Bauer (Lot No. 9007-28-7) and used as supplied. Samples were also obtained from Calbiochem, ICN, Polysciences, Sigma, and SchweitzerHall and put through the same examination mentioned above. Of all these samples, only

that from Pfaltz-Bauer lacked the extraordinary phase, although the Calbiochem sample showed only a weak presence of this phase. As with the Hep, filtering the samples through a 0.1- μm filter permanently removed the extraordinary phase, except in the case of the sample from Sigma which required a 0.05- μm filter.¹⁵

A $dn/dc = 0.15$ was found for both Hep and ChS, and no significant dependence on C_s was seen. The dn/dc measurements were made on a Brice-Phoenix differential refractometer at $\lambda = 436$ nm.

Dialyzed poly(styrenesulfonate) was obtained from Pressure Chemical Co. in the following molecular weights (MW): 35 000, 74 000, 200 000, 780 000, and 1 200 000. The nominal polydispersity in terms of M_w/M_n for all samples was less than 1.1. It should be noted that problems in obtaining accurate dry weights have been reported due to a 5–15% hydration of the highly hygroscopic dry material.¹⁶ Hence, static light scattering is not recognized as a highly accurate method of determining molecular weights for these polymers, since neither dn/dc nor the concentration appearing in the ratio Kc/I can be determined to better than this uncertainty in hydration. Naturally, extrapolation to zero concentration in the Zimm method yields radii of gyration which are independent of dn/dc and c . Our abbreviated method, however, requires both these quantities for determining $\langle S^2 \rangle^{1/2}$. Since we are mostly interested in the relative changes in $\langle S^2 \rangle^{1/2}$ and their comparison to changes in D_0 , such a possible systematic error is not overly troubling.

The EP in NaPSS has been studied by Drifford et al.¹⁷ It has been found recently, however, that this phase could be removed with a 0.05- μm filter,¹⁵ after which it did not reappear on a scale of days.

The incremental refractive index was checked for each molecular weight used at a few selected C_s . At a given C_s , the dn/dc value was found to be constant over the range of molecular weights. An indication was found, however, that dn/dc may have some dependence on C_s and also depended on whether or not the solution was dialyzed against the fixed C_s stock solutions (to achieve chemical equilibrium) before the dn/dc measurements. Since most of the effects investigated in this report depend only on relative quantities, an average was taken over all of the molecular weights and C_s and was found to be $0.189 \pm 5.7\%$, which is in excellent agreement with the value of around 0.189 that Pressure Chemical Co.'s consultants have found.¹⁸

The polyelectrolyte counterions must be included when calculating the total ionic strength, especially at low concentrations of added salt and high concentrations of polyelectrolyte. As the polymer concentration increases, this self-salt effect, which was estimated to be around 1.5 mM/(mg/mL of Hep), 1.4 mM/(mg/mL of ChS), and 0.9 mM/(mg/mL of NaPSS), can add significantly to the total ionic strength. These latter estimates assume that only the counterions not condensed in the Manning sense¹⁸ of $\xi = 1$ contribute to the ionic strength. For the static and dynamic light scattering experiments, care was taken to make extrapolations over low enough C_p regimes where the self-salt effect could be ignored. A rough cross check is afforded by calculating the equivalent C_s of a NaCl based on Hep, ChS, and NaPSS conductivities. The conductivities were found to be 225 $\mu\text{S}/(\text{mg/mL of Hep})$, 201 $\mu\text{S}/(\text{mg/mL of ChS})$, and 175 $\mu\text{S}/(\text{mg/mL of NaPSS})$. By using 160 $\mu\text{S}/(\text{mg/mL of NaCl})$, it was found that the "self-salt" effect amounted to 1.4 mM/(mg/mL of Hep), 1.3 mM/(mg/mL of ChS), and 1.1 mM/(mg/mL of NaPSS) which are in fair agreement with the above estimates based on Manning condensation.¹⁸

It is important to point out that, even if the Manning criterion does not strictly hold for coil molecules, the above self-salt estimates are actually quite unimportant for the zero polymer concentration extrapolations as long as the self-salt contribution to C_s is much smaller than the added electrolyte concentration at the lowest C_p points of the extrapolation.

Additional Observations on the "Extraordinary Phase". Although it is not the principal aim of this work to study the EP, the considerable uncertainty concerning the phenomenon warrants some additional "hard data" and explanatory comments. A separate work dealing exclusively with the EP for a variety of linear polyelectrolytes has recently been submitted.¹⁵

Figure 1a shows D vs C_s for 3 mg/mL of ChS after being filtered through a 0.22- μm filter (lower curve) and after being filtered

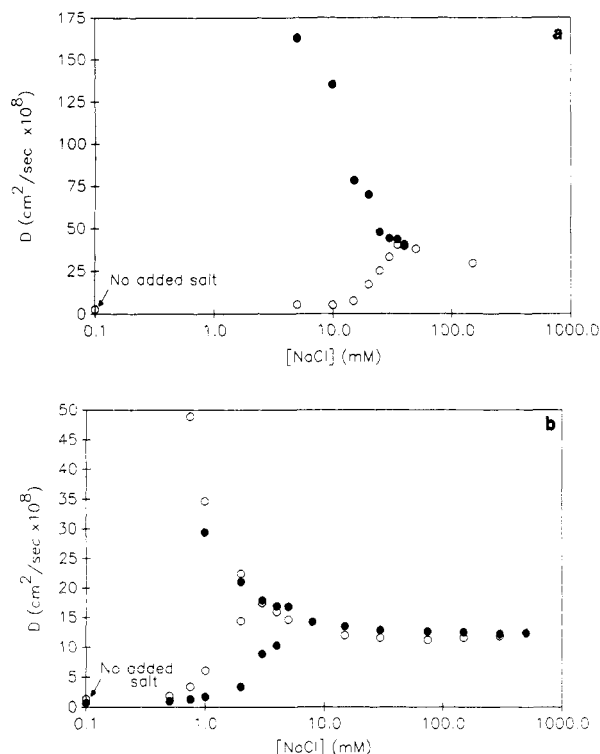


Figure 1. (a) D vs C_s for chondroitin sulfate at 3 mg/mL. Bottom curve (O): the solution was filtered through a 0.22- μm membrane, and "extraordinary phase" behavior is present. Top curve (●): the solution was filtered through a 0.05- μm filter, and no long autocorrelation decay curve was detectable. (b) D vs C_s for 780 000 MW NaPSS at (●) 1 mg/mL and (O) 0.5 mg/mL filtered through a 0.22- μm membrane, showing what is generally considered to be EP behavior. This EP behavior could be permanently removed by filtration through a 0.05- μm membrane.

through a 0.05- μm filter (upper curve). The lower curve, for which D could be obtained even at no added salt ($C_s = 0$), has the behavior of the extraordinary phase reported by many different authors;^{14,17,19} very low D values are obtained at no added salt and very low added salt, which then rise by well over an order of magnitude (about 14 times in this particular case) at higher C_s .

Qualitatively, this solution with the EP is very clean, scatters light very feebly, at a level just above pure water, and is free of the little pinpoints of light characteristic of samples containing "dust" or other impurities. Correspondingly, the autocorrelation function builds up in a smooth manner, as is usual in the case of a well-mixed sample, and does not show the erratic jumps and wide ranges in decay times characteristic of "dust" or other inhomogeneous solutions (inhomogeneous in the sense that the content of the scattering volume in any given moment is not constant; e.g., a "dust" particle may wander in and out).

The percentage loss of material in the upper curve of Figure 1a was 20% as determined by UV absorption. Measurement of scattering intensity by titration to high C_s after filtration and use of eq 1 (see below) with A_2 taken from Figure 3b (see below) gives a loss less than 10%. Thus, the 20% loss is considered a maximum loss. This loss of C_p is insufficient to lower C_p below the level of detectability of the EP. The EP has been observed at C_p far below the slightly reduced C_p resulting from filtration.¹⁵ After filtration through the 0.05- μm membrane it was not possible to autocorrelate the scattered light with no added salt or very low added salt. At $C_s \sim 1$ mM a very fast decaying autocorrelation function was measured, after which D decreased monotonically with increasing C_s . This curve has the hallmarks of what is sometimes termed the "ordinary phase" of diffusion, for which abundant theories exist to account for both electrostatic and hydrodynamic effects in the D vs C_s and D vs C_p behavior. (We suspect that a rapidly decaying autocorrelation function could probably be measured under no and low salt conditions at very low scattering angles, corresponding to the continuing rise of D versus decreasing C_s of the ordinary phase.)

It is on the grounds of the total disappearance of the slow correlation mode after filtration through a certain nominal pore size membrane that it is asserted that the EP has been "removed". This slow mode does not reappear even after days, suggesting that the slow mode corresponds to a nonequilibrium state of the polymer, such as stable aggregates, and does not correspond to, e.g., shear sensitive fleeting associations or networks. It is emphasized that the EP is observed in this work if filtration is performed through large enough pore size membranes, such as 0.22 μm , and sometimes even 0.1 μm . It was found that 0.1- μm and sometimes even 0.05- μm pore size filters were necessary to remove the EP. The conductivities of samples from different manufacturers were found to be quite similar, hence showing that the absence of the EP in a sample prepared "out of the bottle" was not due to an excess of salt. Also, samples of Hep and ChS from different manufacturers were filtered so as to remove the EP and then exhaustively dialyzed (2.5–3 mL sample) against 1800 mL of distilled deionized H_2O ($\sigma < 1 \mu\text{S}$). These samples were then filtered through 0.22- μm filters (which allowed the EP to pass through) so as to remove dust and then investigated as to the presence of the EP. Again, once the EP had been removed, it did not reappear, even after exhaustive dialysis.¹⁵

In case it is surmised that the lower curve of Figure 1a somehow does not represent the EP often observed and reported in the literature, Figure 1b shows the EP behavior of 780 000 MW NaPSS at concentrations of 1 and 0.5 mg/mL (filtered through a 0.22- μm membrane so as to retain the EP), which clearly shows the salient features usually reported: As the C_s increases, the low D increases, the much higher D from the ordinary phase becomes simultaneously measurable, and there is a narrow C_s range over which the low D from the EP rises sharply and disappears. Furthermore, the C_s at which this transition range begins increases with increasing C_p , as is generally reported. Filtering this solution with a 0.05- μm membrane permanently removed all these EP features, leaving only the ordinary phase measurable.

The EP is not being "dismissed" as an artifact such as incomplete elimination of "dust" but rather seems related to a small population of genuine aggregate states of the polyelectrolytes themselves. No claim is made as to the relationship between these removable aggregates and EP observations for systems such as latex spheres. By the same token, since observations of the EP for linear polyelectrolytes have typically been made at concentrations on the order of 1 mg/mL, there is no convincing reason to believe that X-ray and neutron scattering peaks obtained at much higher concentrations (usually > 10 mg/mL) are necessarily related to the EP phenomenon.

Light Scattering. The static and dynamic light scattering equipment included a vertically polarized Coherent argon ion laser operating at 488 nm, a head-on photomultiplier tube, and a Brookhaven BI-2030 autocorrelator. Details of the apparatus and techniques are described elsewhere.²⁰ All light scattering experiments were carried out at 25 $^\circ\text{C}$. Scattering measurements could be made over the angular range $\theta = 30$ – 140° . When multiangle dynamic light scattering scans were made, the sample times were weighted as $\sin^{-2}(\theta/2)$, in order to keep the extent of the autocorrelation decay curve fairly constant from angle to angle. The diffusion coefficients reported are the first cumulant values from the standard power series expansion of the logarithm of the scattered electric field autocorrelation function, obtained from the Gaussian approximation from the homodyne scattered intensity autocorrelation function.

In this study it also proved useful to employ a Wyatt Technology DAWN multiangle static light scattering unit for the radii of gyration measurements on the poly(styrenesulfonate). Agreement of molecular weight between the argon ion and Wyatt system for polystyrene standards was within 3%, so the systems could be used interchangeably for static scattering purposes. The DAWN system, using a vertical 5-mW He–Ne laser, allowed the radii of gyration experiments to be performed at lower values of the scattering vector $q (= (4\pi n/\lambda) \sin(\theta/2))$, i.e., allowing the Zimm plot approximation of $q^2 \langle S^2 \rangle \ll 3$ to be more closely obeyed than for the 488-nm argon ion system. The Wyatt instrument was operated in the "batch mode", that is, using a 20-mL cylindrical scintillation vial as the sample cell.

Estimation of Apparent Persistence Lengths and Excluded Volume. Software was written for the DAWN instrument, which allowed collection and analysis of angular scattering data to yield radii of gyration as a function of salt titration on a single low-concentration sample.

This simple method is similar to the one introduced by Ghosh et al.¹² except that the approximations for the poly(styrene-sulfonate) are fewer and somewhat different. These are as follows:

(1) $q^2 \langle S^2 \rangle \ll 3$ over the entire angular range from 26 to 140°, so that the standard Zimm single contact approximation can be used:

$$Kc/I = (1 + q^2 \langle S^2 \rangle_z / 3) M_w + 2A_2 c Q(\theta) \quad (1)$$

Here I is the angularly dependent Rayleigh ratio, c is the concentration in grams per milliliter, M_w is the weight-averaged molecular weight, A_2 is the second virial coefficient, $Q(\theta)$ is a complicated function of intermolecular interactions, $\langle S^2 \rangle_z$ is the z -averaged mean-square radius of gyration, and

$$K = \frac{4\pi^2 n^2 (dn/dc)^2}{\lambda^4 N_A} \quad (2)$$

where n is the index of refraction of the solvent, λ is the wavelength of the laser in vacuo (632.8 nm), N_A is Avogadro's number, and dn/dc is the incremental refractive index.

(2) At $c < c^*$ (where c^* is the polymer overlap concentration threshold) it was observed experimentally that all isoangular slopes were nearly the same; hence, $Q(\theta) = \text{constant}$, which we set equal to 1.

(3) The population is assumed to be nearly monodisperse, according to the manufacturer's claims.

It then suffices to make a single determination of $I(\theta)$ to obtain $\langle S^2 \rangle$ as

$$\langle S^2 \rangle = 3M \frac{d(Kc/I)}{dq^2} \quad (3)$$

where the subscripts on $\langle S^2 \rangle$ and M have been dropped in light of the low polydispersity of the NaPSS standards. The advantages of this method in this case are (1) it avoids the difficult problem of making truly isoionic dilutions on polyelectrolyte solutions at low ionic strength (because of the self-salt contribution to ionic strength) and (2) at low C_s the polyelectrolyte solutions scatter weakly, so that further dilutions inevitably yield highly scattered data.

The $\langle S^2 \rangle$ thus determined is the perturbed mean-square radius of gyration. It is related to the unperturbed mean-square radius of gyration $\langle S^2 \rangle_0$ by

$$\langle S^2 \rangle = \alpha_s^2 \langle S^2 \rangle_0 \quad (4)$$

where α_s represents the static expansion factor due to electrostatic and hard-core excluded-volume effects. $\langle S^2 \rangle_0$ (the value if no excluded-volume effects were present) is related to the polymer contour length L and the total persistence length L_T through the wormlike chain model by

$$\langle S^2 \rangle_0 = LL_T/3 - L_T^2 + 2L_T^3/L - 2(L_T^4/L^2)[1 - \exp(-L/L_T)] \quad (5)$$

L_T is comprised of the intrinsic persistence length L_0 and the electrostatic persistence length L_e , such that $L_T = L_0 + L_e$. The Odijk²¹ and Skolnick/Fixman²² theory for L_e gives

$$L_e = (QN^2/12)[3y^{-2} - 8y^{-3} + e^{-y}(y^{-1} + 5y^{-2} + 8y^{-3})] \quad (6)$$

where Q , the Bjerrum length, is $q^2/d_e k_B T$ (about 7.2 Å at 25 °C), q being the size of the individual charges and d_e the dielectric constant of the solution, $y = \kappa L$ where κ^{-1} is the Debye screening length, and N is the number of charged units in the chain.

If the experimental $\langle S^2 \rangle$ obtained from eq 3 is used in place of $\langle S^2 \rangle_0$ in eq 5, then the L_T so determined is an "apparent persistence length"¹² and is designated hereafter as L_T' . It implicitly includes all electrostatic and "hard" excluded-volume effects and provides an upper limit on L_T . The extrapolation of L_T' to infinite ionic strength yields the apparent intrinsic persistence length L_0' . Subtracting L_0' from L_T' at any ionic strength yields the apparent electrostatic persistence length L_e' ($L_T' = L_0' + L_e'$).

Several recent works have shown that combining different current theories of electrostatic excluded volume^{23,24} with the unperturbed electrostatic persistence length theory of Odijk and Fixman and Skolnick gives a fair fit to the $\langle S^2 \rangle$ values determined by light scattering^{12,13} and Monte Carlo results^{25,26} and hence is at least partially successful in accounting for the observed approximate power law.

For a polyelectrolyte in low to moderate C_s , the steric interactions may be much less than the electrostatic interactions on the total excluded volume. It has been proposed that polyelectrolytes which behave like wormlike chains may be approximated by random coils with $N_k = L/2L_T$ Kuhn segments of length $L_k = 2L_T$ and that the excluded volume can then be treated by the standard excluded-volume parameter z

$$z = (3/2\pi L_k^2)^{3/2} \beta N_k^{1/2} \quad (7)$$

where $\beta = \beta_0 + \beta_{el} + \beta_a$ is the sum of hard-core repulsion, electrostatic, and attractive excluded-volume terms, respectively, between the segments.²³ Fixman and Skolnick²⁴ found a form for the binary cluster integral β_{el} , due to electrostatically interacting rods as

$$\beta_{el} \simeq 8L_T^{-2} \kappa^{-1} R(w) \quad (8)$$

where $w = 2\pi \xi^2 Q^{-1} \kappa^{-1} \exp(-\kappa d)$, d being the cylinder diameter, and

$$R(w) = \int_0^{\pi/2} \sin^2 \theta \int_0^{w/\sin \theta} x^{-1} (1 - e^{-x}) dx d\theta \quad (9)$$

The excluded-volume parameter, z , may then be used to calculate the expansion factor, α_s . In the case where the polyelectrolyte has more than two Kuhn segments, the Gupta-Forsman equation²⁷

$$\alpha_s^5 - \alpha_s^3 = (134/105)(1 - 0.885N_k^{-0.462})z \quad (10)$$

has been found to often yield the best correction.²⁵ Below $N_k = 2$, the modified Flory equation can be resorted to:^{28,29}

$$\alpha_s^5 - \alpha_s^3 = \frac{134}{105} z \quad (11)$$

Steric or hard monomer excluded volumes are not included in eqs 8 and 9, so that the α_s computed from eqs 10 or 11 based on eqs 7–9 is due solely to electrostatic effects. The large positive values of A_2 suggest that the attractive part of the excluded volume, β_a , is negligible.

Once α_s and z are found, one can then extend the notion of electrostatic excluded volumes to the calculation of the second virial coefficient, A_2 , by Yamakawa's²⁹ equation (21.5)

$$A_2 = (N_A N_k^2 \beta / 2M^2) h_0(z) \quad (12a)$$

where

$$\bar{z} = z/\alpha_s^3 \quad (12b)$$

is an approximation introduced by Yamakawa to account for the effect of intramolecular excluded volume on A_2 and

$$h_0(\bar{z}) = [1 - (1 + 3.903\bar{z})^{-0.4683}]/1.828\bar{z} \quad (12c)$$

Tanford³⁰ gives β_0 of a hard rod of length L and diameter d as

$$\beta_0 = \pi d L^2 / 2 \quad (13)$$

For random coils whose cylindrical segment lengths are L_k , the hard-core contribution to A_2 in eq 12a is

$$A_{2, \text{hard}} = N_A N_k^2 \beta_0 h_0(z) / 2M^2 \quad (14a)$$

$$\propto L^2 h_0(z) / M^2 \quad (14b)$$

Since the electrostatic contribution to A_2 rapidly becomes much larger than $A_{2, \text{hard}}$ and $h_0(\bar{z})$ is a function slowly decaying from 1.0 as \bar{z} increases, A_2 can be approximated by

$$A_2 \approx N_A N_k^2 \beta_{el} h_0(\bar{z}) / 2M^2 + A_{2, \text{HS}} \quad (15)$$

where $A_{2, \text{HS}}$ is the value of A_2 extrapolated to infinite ionic

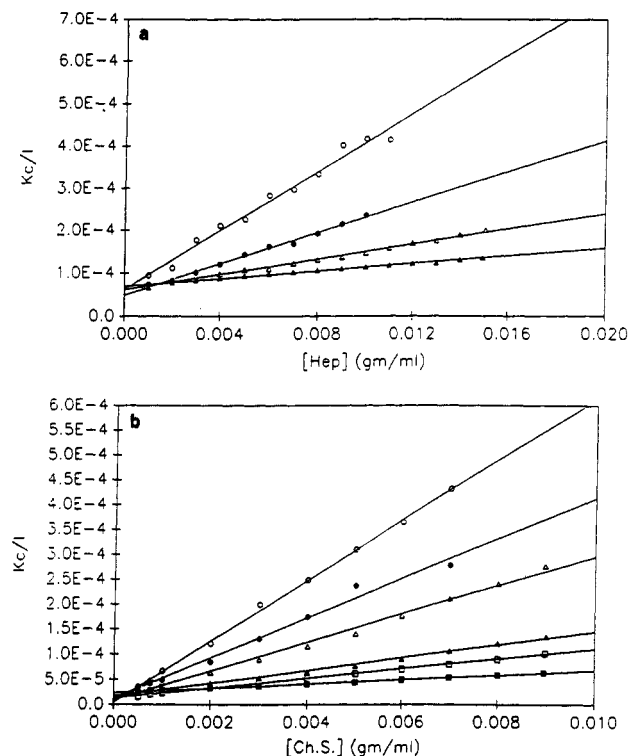


Figure 2. (a) Kc/I vs $[Hep]$ at $\theta = 90^\circ$ in (○) 15, (●) 50, (Δ) 150, and (□) 1000 mM NaCl. (b) Kc/I vs $[ChS]$ at $\theta = 90^\circ$ in (○) 10, (●) 15, (Δ) 30, (▲) 100, (◻) 150, and (■) 1000 mM NaCl.

strength. Using eqs 7 and 10 and $A_{2,HS}$ in eq 12a with $\beta = \beta_0$ allows the hard-core expansion factor at high salt $\alpha_{s,HS}$ to be found. This in turn allows an estimate of the true intrinsic persistence length, which in the coil limit is

$$L_0 = L_0' / \alpha_{s,HS}^2 \quad (16)$$

Results and Discussion

Heparin and Chondroitin 6-Sulfate. Static light scattering on Hep in NaCl was done over an extended angular range ($50^\circ \leq \theta \leq 140^\circ$). No angular dependence was found. Each angle was analyzed separately, using linear fits over the lower concentration regions where the data appeared to be linear. Except at the very lowest salts, it was found that A_2 had little or no angular dependence, suggesting that $Q(\theta)$ was a constant and was taken to be equal to 1 in eq 1. Figure 2a shows Kc/I vs c for different values of C_s at $\theta = 90^\circ$. The molecular weight was approximately 16 000. The second virial coefficients are shown in Figure 3a. These agreed fairly well with those found for high-affinity Hep by other researchers.³¹⁻³³

Static scattering on ChS over $30^\circ \leq \theta \leq 140^\circ$ showed a very slight angular dependence. This weak dependence led to small values of $\langle S^2 \rangle^{1/2}$ whose error bars, however, were too large to reliably observe trends. Kc/I at several different C_s at $\theta = 90^\circ$ are shown in Figure 2b. Values of A_2 are shown in Figure 3b. In parts a and b of Figure 2 the lowest C_p data points for the $C_p = 0$ extrapolations are low enough that the "self-salt" is much less than the added salt concentration. A molecular weight of 70 000 was found. This molecular weight is in good agreement with previous studies.^{34,35} The second virial coefficients, however, were found to be higher than those found by other researchers.³⁵⁻³⁷

A_2 calculations based on eqs 6-10, 12, and 15 and on eq 13 were made. In all cases, the calculations radically diverged from the experimental data at low ionic strength,

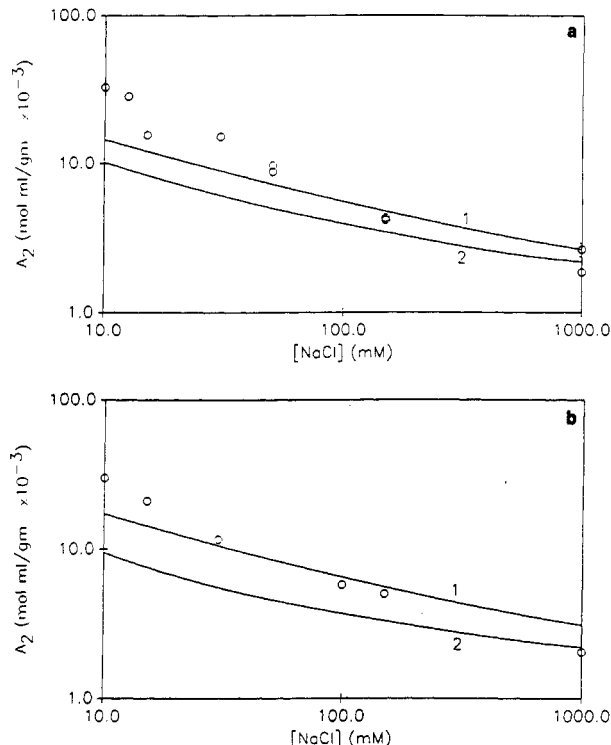


Figure 3. (a) A_2 vs C_s for Hep with calculations using (1) eq 13 and a hard radius of 3 Å and (2) eqs 6-10, 12, and 15. (b) A_2 vs C_s for ChS with fits using (1) eq 13 and a hard radius of 3 Å and (2) eqs 6-10, 12, and 15.

even with $L_0 = 500$ Å, as can be seen in parts a and b of Figure 3. A linear fit on the data yielded a slope of just over -0.5 for both Hep and ChS and, as it turns out, for HA as well.¹²

The diffusion coefficients of Hep and ChS showed no angular dependence. This reflects both the fact that $P(\theta)$ is nearly unity for Hep and ChS, and the absence of any influence from internal flexional modes of the polymers on the autocorrelation decay function. It was thus sufficient to measure D of Hep and ChS at $\theta = 90^\circ$. D vs $[GAG]$ was measured at constant added C_s using NaCl and, in the case of Hep, using $CaCl_2$ and histamine as well. These are shown in parts a-c of Figure 4. The data from Figure 4a at $[Hep] = 15$ mg/mL agrees reasonably well with that obtained by Tivant et al.,³⁸ at low C_s , although it is a little bit higher than their result at 1000 mM NaCl. Remarkably, for ChS, the extrapolated zero-concentration diffusion coefficient, D_0 , is independent of C_s . For Hep, D_0 is not only independent of C_s but also independent of whether mono- or divalent salts are used. In conformity with the established interpretations of the homodyne scattered intensity autocorrelation function of dynamic light scattering, we take the zero polymer concentration intercept of D , D_0 , to represent the self-diffusion coefficient of the polymers, i.e., to measure the friction of a single polymer molecule in the solvent.

The surprising result that D_0 is independent of C_s for heparin and chondroitin sulfate mirrors the result for HA¹² and NaPAA.¹³ For HA and NaPAA, a comparison of D_0 (extrapolated to both $\theta = 0^\circ$ and $C_p = 0$) at different NaCl concentrations and the radii of gyration, $\langle S^2 \rangle^{1/2}$, at these salt concentrations showed that, as $\langle S^2 \rangle^{1/2}$ changed, the diffusion coefficient stayed the same, suggesting that HA and NaPAA are at least partially draining.^{12,13} Even though $\langle S^2 \rangle^{1/2}$ could not be measured for Hep and ChS, the result seen for D_0 and the fact that the GAG structures are similar would also seem to imply that both Hep and

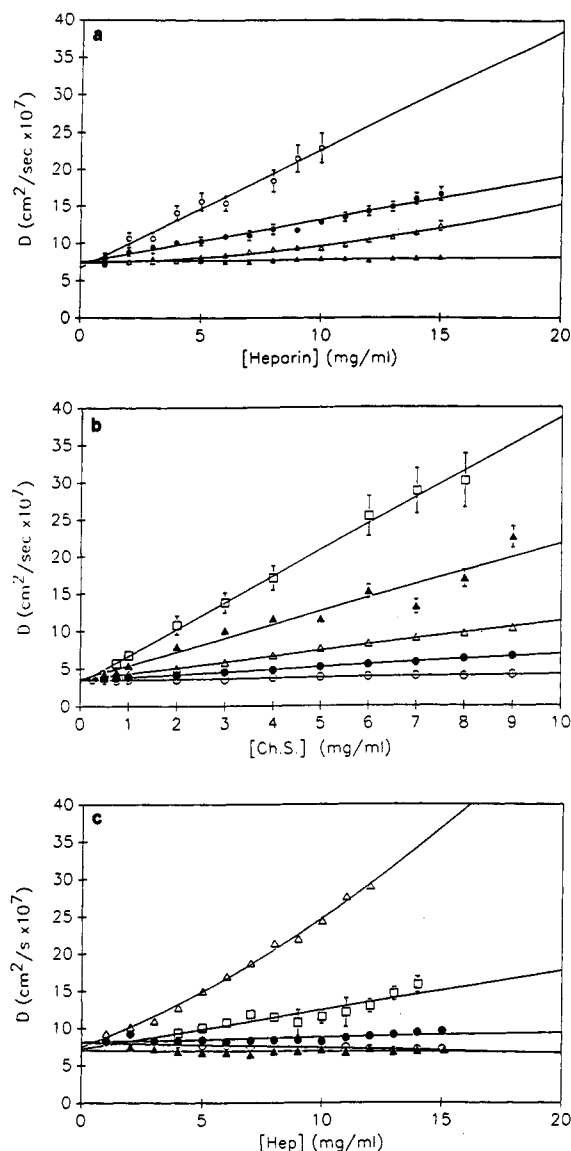


Figure 4. (a) D vs [Hep] at $\theta = 90^\circ$ in (○) 15, (●) 50, (Δ) 150, and (▲) 1000 mM added NaCl. (b) D vs [ChS] at $\theta = 90^\circ$ in (□) 5, (▲) 10, (Δ) 15, (●) 50, (○) 150 and (○) 1000 mM added NaCl. (c) D vs [Hep] at $\theta = 90^\circ$ in (Δ) 10, (○) 50, and (●) 1000 mM CaCl_2 as well as (□) 10 and (▲) 600 mM histamine.

Table I
Experimental and Calculated D_0 for Hep and ChS^a

	$D_0, \times 10^7 \text{ cm}^2/\text{s}$			
	Hep		ChS	
	15 mM C_s	1000 mM C_s	15 mM C_s	1000 mM C_s
exptl, %	7.44 ± 2.3^b		3.27 ± 11^c	
no excluded vol. ^d	9.1	10.1	3.01	4.01
with excluded vol. ^e	7.62	9.98	2.23	3.86

^a The calculated values use eqs 17 and 18 in combination first with no excluded-volume correction and then by using eq 10. Values are given at 15 and 1000 mM C_s . ^b From the $C_p = 0$ intercept of Figure 4a,c. ^c From the $C_p = 0$ intercept of Figure 4b. ^d By eqs 17 and 18 with $L_T = 21.3 \text{ Å} + L_e$; L_e by eq 6 ($N_k = L/2L_T$, $L = 265 \text{ Å}$ for Hep, and $L = 1390 \text{ Å}$ for ChS). ^e By eqs 17 and 18 with L_T' calculated by eqs 7–10.

ChS likewise exhibit some draining. Significantly, similar studies on proteoglycan monomers showed that they behaved in the putative nondraining limit, with $R_h \sim 0.7\langle S^2 \rangle^{1/2}$ over the 1–1000 mM range of C_s .³⁰ Thus, it was concluded that the obtention of a C_s -independent D_0 was not merely an artifact of the light scattering methodology.

That the D_0 independence from C_s probably does not result from total free draining can be surmised by the very rough $1/D_0 \propto M^{0.4}$ dependence afforded by the Hep and ChS data. Because of polydispersity and the fact that Hep and ChS are not identical, we do not take the 0.4 exponent as precise but rather as an indication that $1/D_0$ does not scale as M , as would be expected for total free draining.

Ranges on the frictional factors, and hence the diffusion coefficients, were estimated in the nondraining limit using Davis and Russel's⁴⁰ polyelectrolyte interpretation of the Yamakawa and Fujii¹ expression for the frictional coefficient f_0 for an unperturbed wormlike chain of rod diameter d , contour length L , and a number of Kuhn lengths N_k . For N_k greater than 2.278

$$3\pi\eta_0 L/f_0 = 1.843N_k^{1/2} + a_2 + a_3N_k^{-1/2} + a_4N_k^{-1} + a_5N_k^{-3/2} \quad (17)$$

In the case of $N_k < 2.278$

$$3\pi\eta_0 L/f_0 = b_1 \ln(N_k/h) + b_2 + b_3N_k + b_4N_k^2 + b_5N_k^3 + b_6 \frac{h}{N_k} \ln(N_k/h) \quad (18)$$

here η_0 is the viscosity of the solvent.⁴⁰ The frictional coefficient f_0 is related to D_0 by way of the Einstein relation, $f_0 = k_B T/D_0$. The coefficients, $a_2 \dots a_5$ and $b_1 \dots b_5$, which are functions of d/L_k , are given in ref 40.

Equations 17 and 18 were used to calculate D in the case of no excluded volume by taking $N_k = L/2L_T$, with $L_T = L_0 + L_e$ where $L_0 = 21.3 \text{ Å}$ ³¹ and L_e was calculated by eq 6. The contour length L used was 265 Å for Hep and 1390 Å for ChS. Table I shows experimental values of D_0 for Hep and ChS at 15 and 1000 mM C_s . In addition, values of D at these same ionic strengths calculated in the case of no excluded volume, as well as including the influence of excluded volume by using eqs 6–10 to calculate α_s , are shown. The effect of the excluded volume on D_0 was made under the assumption that the relative changes in the friction factor ($f = \alpha_H f_0$, where α_H is the hydrodynamic expansion factor) can be found with $\alpha_s/\alpha_H = \text{constant}$, which is only necessarily true in the nondraining limit.

Davis and Russel⁴⁰ noted that their theoretical predictions constantly underpredict the frictional coefficient (and hence overpredict the diffusional coefficient) by as much as 40%, with the largest differences occurring as θ conditions are approached. In our case, the deviations from the prediction may also be related to the Hep and ChS polydispersity, for which we attempt no corrections. At any rate, with or without excluded volume, eqs 17 and 18, based on strong hydrodynamic interactions, predict changes in D_0 that are larger than the error bars of the C_s -independent D_0 's found.

Poly(styrenesulfonate). Figure 5a shows typical behavior for Kc/I vs q^2 for 0.1 mg/mL NaPSS of $M = 780\,000$ at different values of C_s . At this concentration, the self-salt is only 0.09 mM, which is negligible even at the lowest C_s shown, 2 mM. The corresponding $\langle S^2 \rangle$ are shown vs $C_s^{-0.5}$ in Figure 5b. The right-hand side of Figure 5b shows L_T' , the apparent total persistence length as calculated by eq 5, using the measured $\langle S^2 \rangle$ instead of $\langle S^2 \rangle_0$. To calculate L_T' , a contour length of $L = 9646 \text{ Å}$ was used for the 780 000 MW NaPSS, which assumes a monomer weight of 207 and a monomer contour length of 2.56 Å. The high salt limit of $L_0 \approx 31 \text{ Å}$ represents the apparent intrinsic persistence length L_0' due to the inherent "stiffening" factors such as bond angle, energetically differently weighted rotameric states, hard-core

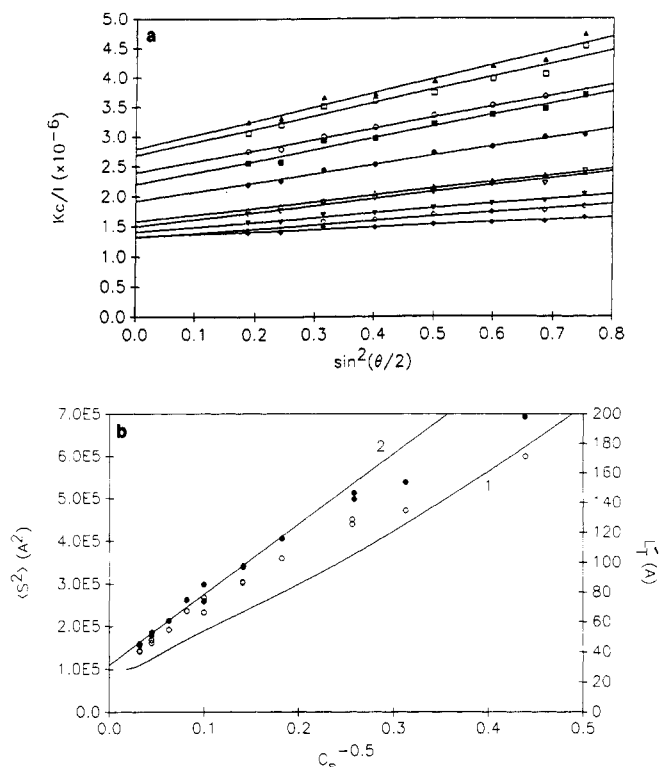


Figure 5. (a) Kc/I vs $\sin^2(\theta/2)$ for 780 000 MW NaPSS in (\blacktriangle) 1.5, (\square) 2, (\circ) 2.5, (\blacksquare) 5, (\bullet) 10, (\triangle) 15, (∇) 30, (\blacktriangledown) 50, (\diamond) 100, and (\blacklozenge) 1000 mM NaCl. (b) $\langle S^2 \rangle$ vs $C_s^{-0.5}$ for 780 000 MW NaPSS. L_T' on the right-hand axis. (\circ) Experimental $\langle S^2 \rangle$ data. (\bullet) Associated L_T' . Also shown are (1) calculation for $\langle S^2 \rangle$ using eqs 6–10 and (2) a linear fit of L_T' over the low $C_s^{-0.5}$.

excluded volume, etc. This value of L_0' seems somewhat higher than that in other reports, but it and indeed the slope of L_T' vs $C_s^{-0.5}$ are all in reasonable agreement with the results of Tricot, who applied the Yamakawa expression for the viscosity of wormlike chains⁴¹ to the viscosity data in the literature. Between 2 mM and 4 M C_s there are thus at least 14–126 Kuhn segments (since L_T' is an upper limit on L_T); i.e., the NaPSS is never in the rod limit for this range.

The motivation for plotting L_T' vs $C_s^{-0.5}$ is that the maximum linear correlation coefficient when fitting the L_T' data to the expression $L_T' = L_0' + C_s^\nu$ is obtained around $\nu = -0.5$. The maximum, however, is fairly broad and ranged as low as -0.35 when L_T' points down to $C_s = 1$ mM were included, so only an approximate inverse square relationship between L_T' and C_s is asserted. Deviations of L_T' from linearity at high $C_s^{-0.5}$ may be due to a changing dn/dc with C_s , which was not taken into account in the computations. There have been a number of works recently which have shown this type of approximate inverse square root behavior for a number of different polyelectrolytes.^{12,13,41} By using a linear fit over the C_s range 4–4000 mM, one obtains a linear expression for $\langle S^2 \rangle$ (in \AA) vs $C_s^{-0.5}$ for the 780 000 MW NaPSS

$$\langle S^2 \rangle (\text{\AA}^2) = 1.01 \times 10^5 + 1.45 \times 10^6 C_s^{-0.5} \quad (19)$$

and for L_T' (in \AA)

$$L_T' = 31.3 \text{\AA} + 472.1 \text{\AA} \text{ mM}^{1/2} \times C_s^{-0.5} \quad (20)$$

C_s is expressed in millimolar in eqs 19 and 20.

The attempt to calculate the second virial coefficients for 780 000 MW NaPSS using eqs 7–15 yielded an almost exact match to the data. Figure 6 shows the experimental second virial coefficients for the 780 000 MW NaPSS as

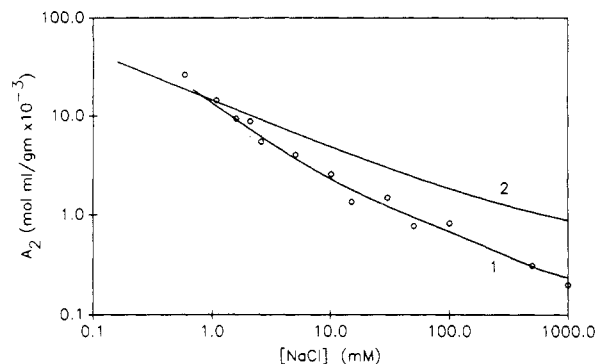


Figure 6. Experimentally obtained A_2 vs C_s for 780 000 MW NaPSS as well as theoretical calculations utilizing (1) eqs 6–10, 12, and 15 and (2) eq 13.

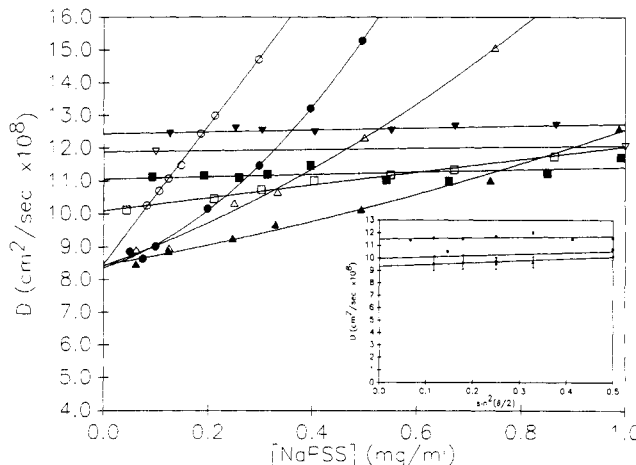


Figure 7. D vs [780 000 MW NaPSS] in (\circ) 2, (\bullet) 5, (\triangle) 7.5, (\blacktriangle) 30, (\square) 150, (\blacksquare) 500, (∇) 1000, and (\blacktriangledown) 4000 mM NaCl. The inset shows D vs $\sin^2(\theta/2)$ for $C_p = 0.1$ mg/mL at $C_s =$ (\circ) 2, (\triangle) 10, and (\bullet) 500 mM.

well as calculated values using eqs 6–10, 12, and 15. The extrapolation of A_2 vs $1/C_s^{0.5}$ to infinite ionic strength yielded $A_{2,HS} = 0.7 \times 10^{-4} - 1.1 \times 10^{-4}$. Since $\beta_{el} = 0$ at infinite ionic strength, the hard-core expansion factor in that limit is $\alpha_{s,HS} \approx 1.07 - 1.1$, which gives a true intrinsic persistence length L_0 of 23–27 \AA for NaPSS.

Figure 7 shows D vs C_p for the same 780 000 MW NaPSS at selected values of C_s for $\theta = 90^\circ$. At all C_p and C_s , D was independent of θ from 90° to 30° . The inset in Figure 7 makes this explicit by showing D vs $\sin^2(\theta/2)$ for 0.1 mg/mL of 780 000 MW NaPSS at $C_s = 2, 10, \text{ and } 500$ mM. The error bars on these points (not shown) range from about $\pm 2\%$ at high C_p , where autocorrelation curves were easily obtained, to about $\pm 6\%$ at the low C_p and low C_s , where autocorrelation was more difficult. From the inset in Figure 7, it can be seen that, over the range of $0^\circ \leq \theta \leq 90^\circ$, D has virtually no angular dependence. At 2 mM C_s , the change in D amounts to about 5.5%, at 10 mM C_s , the change in D is about 7.5%, and at 500 mM C_s , this change is about 1.6%. The average slope over this range of C_s is only 0.86×10^{-8} . (The equation $D_{app} = D_0(1 + C \langle S^2 \rangle q^2)$, based on internal modes, where D_{app} is the apparent diffusion coefficient and $C = 0.2$ for a random coil,⁴² would predict an angular change in D_{app} of 19.3% at $C_s = 500$ mM, 55% at 10 mM C_s , and 95% at 2 mM C_s . Such slopes are clearly absent.) Thus, the contribution of any internal modes to D is not measurable over $30^\circ \leq \theta \leq 90^\circ$. At the low C_s , however, it has been noted that there is a very slight rise in D at angles above about 120° . Thus, under the extremes of low C_s (high coil expansion)

Table II
Experimental Values of $\langle S^2 \rangle^{1/2}$ and R_H for
780 000 MW NaPSS in 2, 15, and 4000 mM C_s ^a

	2 mM C_s	15 mM C_s	4000 mM C_s
exptl $\langle S^2 \rangle^{1/2}$, Å	901	686	351
exptl R_H , Å	290	289	196
$\langle S^2 \rangle^{1/2}/R_H$	3.11	2.37	1.79
calc R_H , no excluded vol., Å	405	247	196
calc R_H using eq 10, Å	556	380	196

^a Also shown are the ratios between the two. In addition, values of R_H calculated using eqs 17 and 18 without the excluded-volume correction and then by using eq 10 are given.

and high θ (well above the 90° used for the extrapolations to $C_p = 0$ in Figure 7) there may be some small influence of polydispersity and/or internal modes appearing in the autocorrelation function. As the extrapolations to $C_p = 0$ are independent of those small high- q and low- C_s effects, however, the interesting topic of internal modes is not pursued here.

The $C_p = 0$ intercepts of Figure 7, which represent the diffusion coefficients after all interactions between polymers have been removed, D_0 , are seen to depend on C_s in a complicated way. At and below about $C_s = 30$ mM, D_0 is independent of C_s , just as it was for ChS and Hep at all C_s . Unlike Hep and ChS, however, above 30 mM D_0 becomes a function of C_s .

Table II shows $\langle S^2 \rangle^{1/2}$ and $R_H (=k_B T/6\pi\eta D_0)$ for NaPSS in 2, 15, and 4000 mM C_s , as obtained experimentally. This ratio is not constant over the range of C_s shown in Figures 5b and 7. At 2 mM C_s $\langle S^2 \rangle^{1/2}/R_H = 3.11$ and at 15 mM this ratio is 2.37, while at 4000 mM C_s it is equal to 1.79. This latter value is not too far from the 1.47 ratio predicted in the nondraining limit. This suggests there is some change in the draining characteristics of the NaPSS. In addition, Table II shows R_H at these three C_s as calculated using eqs 17 and 18 first without any excluded-volume correction and then by using eq 10.

The relationship between the static expansion factor α_s and the hydrodynamic expansion factor α_H is a controversial topic and the subject of much theoretical activity.^{3,7,10,43,44} It is beyond the scope of this paper to review the subject here. Briefly, experimental evidence for the nonuniversality of the ratio α_s/α_H has been found,^{13,44} and theories have been elaborated which treat the dependence of α_H on excluded volume and draining parameters.^{3,7,44} A qualitative argument prefacing a theoretical treatment by Wang et al.³ states that the frictional factor f may be expected to increase at less than the proportionality rate of M^ν , $\nu > 0.5$, at which $\langle S^2 \rangle^{1/2}$ increases, i.e., that α_s/α_H is not constant. This is because as the polymer dimension increases with mass in a non-Markov fashion due to the excluded-volume effect, solvent may be expected to begin to drain through the outer layers of the coil. In the absence of draining, however, Douglas and Freed assert that α_s must be proportional to α_H from the viewpoint of renormalization group theory.⁷

In fact, the data shown in Figures 5a and 8a and provided by Table II provide vivid evidence that α_s/α_H is not constant. In Figure 8a, the D_0 data for 780 000 MW NaPSS is plotted as equivalent hydrodynamic diameter $D_H (=k_B T/3\pi\eta D_0)$ vs C_s together with the high C_s value of D_H , 393.2 Å, scaled by the ratio of $\langle S^2 \rangle^{1/2}$ at each C_s to the $\langle S^2 \rangle^{1/2}$ at 4 M C_s , 351 Å, taken from Figure 5b; i.e., this scaled curve represents the expected variation in D_H if α_s/α_H remained constant and is scaled to unity over the 2–4000 mM range of C_s for convenience. This is true since the light scattering values of the mean-square radius of gyration $\langle S^2 \rangle$ are actually of the perturbed values

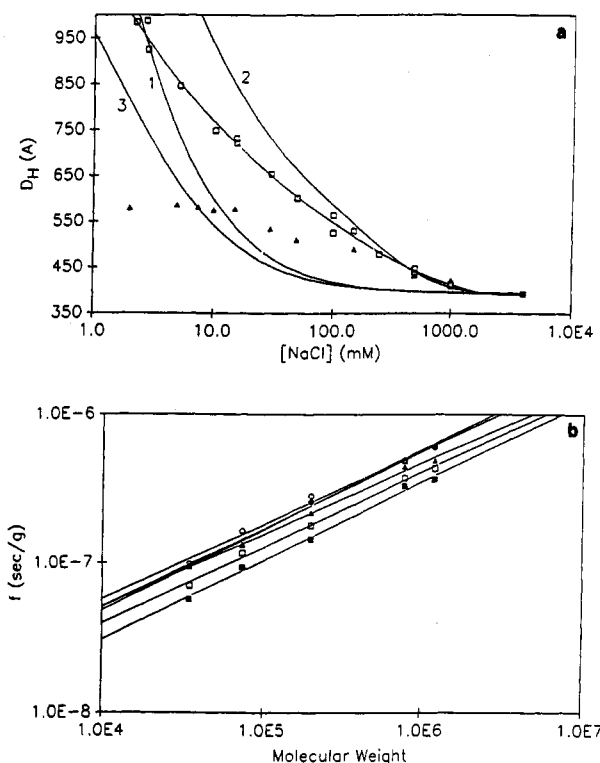


Figure 8. (a) D_H vs C_s for 780 000 MS NaPSS. The experimentally obtained intercepts (Δ) are shown along with the predicted non-free-draining intercepts (\square) using the experimental values of $\langle S^2 \rangle^{1/2}$ from Figure 5a for scaling the experimental intercept at 4000 mM NaCl. Also shown are the predicted non-free-draining intercepts using theoretical values for $\langle S^2 \rangle^{1/2}$ to scale the experimental intercept at 4000 mM C_s in the case of (1) no excluded volume and (2) using eqs 7–10. Finally, (3) the theoretically predicted nondraining intercepts using eqs 17 and 18 with no excluded volume correction are shown. (b) $\log(f)$ vs $\log(M)$ for NaPSS in (○) 5, (●) 10, (▲) 15, (▲) 75, (□) 500, and (■) 4000 mM NaCl.

$\alpha_s^2 \langle S^2 \rangle_0$. In addition to the nondraining predicted curve using the experimental data from Figure 5B, a curve using this same scaling is shown using only eq 6 for the electrostatic persistence length (and no excluded volume). A second theoretical curve is also shown which does take into account the electrostatic excluded volume by using eqs 7–10. A third calculation using eqs 6, 17, and 18 without any excluded-volume correction is also shown.

While aimed primarily at studying semidilute solution behavior, the sparse data for very dilute D by Koene et al.^{45–47} on different molecular weight NaPSS are in good agreement with the current data. The common D_0 for the 780 000 MW NaPSS found at and below 30 mM C_s in the study presented here, 8.48×10^{-8} cm²/s, agrees fairly well with the low concentration result in ref 45 for 10 mM C_s . In ref 47, our $C_p = 0$ extrapolation of their D_0 data for the 650 000 MW NaPSS in 10 mM C_s and in 25 mM C_s also seems to indicate a common intercept. Except for their result for the 1 200 000 MW NaPSS, which was quite a bit lower than that reported here, we find that their low concentration D_0 data also scale by the 0.5 power law seen in Figure 8b.

As the overlap concentration c^* (where a polymer solution nominally passes into the semidilute regime) is important in considering over what range of C_p extrapolations to $C_p = 0$ may be considered valid, the estimate of $c^* \sim 3M/(4\pi \langle S^2 \rangle^{3/2} N_A)$ can be used. Then, for NaPSS at 5 mM ($\langle S^2 \rangle = 7 \times 10^{-11}$ cm²) $c^* \sim 0.5$ mg/mL, whereas at 4000 mM C_s ($\langle S^2 \rangle = 1.5 \times 10^{-11}$ cm²) $c^* \sim 5.0$ mg/mL. Thus, the extrapolations to $C_p = 0$ shown in Figure 7 are

performed over a range where $C_p \ll c^*$. This also strengthens the use of assumption 2 in Estimation of Apparent Persistence Lengths and Excluded Volume.

If the range of C_p is not low enough for the extrapolations to $C_p = 0$, then erroneous conclusions concerning D_0 vs C_s may be reached. Recently, for example, D_0 , extrapolated to $\theta = 0^\circ$, was also found independent of C_s for variably ionized NaPAA.¹³ Extrapolations used C_p values as low as 0.04 mg/mL. By contrast an earlier report⁴⁸ on similar NaPAA truncated the extrapolation at $C_p \sim 0.3$ mg/mL (except for a few aberrant points at lower C_p), which led to the conclusion that D_0 depended on C_s and ξ the way one would expect for polyelectrolyte expansion and contraction in response to these factors. Premature truncation of the D vs C_p extrapolations in ref 13 at $C_p \sim 0.3$ mg/mL would have led to the same erroneous conclusions. Likewise, in Figure 7 of the present work, it can be seen that truncating the D vs C_p extrapolations at, say, 0.3 mg/mL would likewise lead to seriously different conclusions concerning D_0 vs C_p ; e.g., there would no longer be a plateau of D_0 vs C_s at low C_s .

Qualitatively, it does not seem difficult to rationalize the extreme divergence between the average static dimension $\langle S^2 \rangle$ and the frictional factor. For a given mass the swelling of the polyelectrolyte is taking place due purely to electrostatic effects. Whether these are taken as a combination of an unperturbed L_e' due to local electrostatic stiffening as given by eq 6, further enhanced by the electrostatic excluded-volume effects, or whether the net swelling is treated as the balance between electrostatic swelling balanced by an entropic "restoring force" does not matter. The net expansion is due to "soft" forces (electrostatic and entropic) which would not be expected to directly interact hydrodynamically with solvent molecules the same way the hard-core steric exclusion of the monomer masses should. Hence, one might think that there is a certain "hydration sheath" about the polyelectrolyte of finite extent (say, 10–30-Å diameter) which, together with the monomers provides effective hard resistance to the flow of solvent molecules. When the polymer begins to open due to electrostatic effects, a certain state of expansion should be reached at which solvent flows by this hard volume, and though while this still leads to perturbed flow at spatially removed points, the polymer ceases to be fully nondraining. The polyelectrolyte chain at some point might become hydrodynamically "indifferent" to further electrostatically based coil expansion, e.g., as in Figure 4a–c for all C_s and in the plateau at low C_s in Figure 8a.

The problem with this latter view is that after the D_0 vs C_s plateau is reached the polymer would seem to be fully draining, which would then imply that f should scale linearly with M in the plateau region. Figure 8b shows $\log(f)$ vs $\log(M)$ for NaPSS solutions at different C_s . The exponent for the scaling relation $1/D_0 \propto M^\nu$ is 0.5 within error bars for all C_s .

Hence, no matter how tempting it is to assign the interpretations of free draining, partial draining, and non-draining to the three C_s regimes in Figure 8a, the mass scaling data seem to contradict at least the interpretation of free draining. It is not clear what complex set of interactions would or could lead to such a fortuitous cancellation to produce the plateau region at low C_s or indeed at all C_s for Hep, ChS, HA, and NaPAA. Presumably some draining effect is implicated in the phenomenon, probably not full free draining because of the conflict with the mass scaling data. What seems certain is that f does not follow $\langle S^2 \rangle^{1/2}$, so that diffusion coefficient

measurements by dynamic light scattering may not be a valid way of sizing all linear polyelectrolytes in medium to low C_s ranges.

That the plateau is not merely due to the 780 000 MW NaPSS reaching the rod limit seems clear. First of all, the L_T' of 112 Å at the onset of the plateau at around 30 mM C_s is an upper limit on L_T , so there are at least 45 Kuhn segments in the chain, which in fact brings it close to the coil limit. Second, for a rod

$$\langle S^2 \rangle^{1/2} = L/\sqrt{12} \quad (21)$$

which yields $\langle S^2 \rangle^{1/2} = 2785$ Å. The highest value measured was 934 Å at 1.7 mM C_s .

Finally, it is reemphasized that, as in the case of previous reports of the independence of D_0 from C_s for HA¹² and NaPAA,¹³ the effect is not due to an angular dependence of D on θ (see inset in Figure 7). A slight rise in D at very high θ and low C_s may be related to internal flexional modes (and/or polydispersity), and while this does not effect the extrapolations of D to $C_p = 0$ made at $\theta = 0^\circ$, internal modes in principle are related to such macromolecular stiffness and intramolecular hydrodynamic interactions.^{19,42} Thus, studies of internal modes per se might help to further clarify the hydrodynamic effects obtained in this work.

Conclusion

Zero polymer diffusion coefficients D_0 were independent of C_s over the range 5–1000 mM for both chondroitin 6-sulfate and heparin. This, in combination with the results found previously for bacterial hyaluronate,¹² suggests some type of partial-draining condition for these GAGs.

Determining the behavior of both $\langle S^2 \rangle$ and D_0 vs C_s for NaPSS shows that f is independent of $\langle S^2 \rangle^{1/2}$ in solutions up to about 30 mM C_s , likewise suggesting some type of draining condition. At 30 mM C_s , L_T' is about 112 Å. From about 30–100 mM C_s there is a transition region of less draining, after which the nondraining limit is reached ($f \propto \langle S^2 \rangle^{1/2}$).

Why NaPSS exhibits these different regimes, whereas Hep, ChS, bacterial HA,¹² and variably ionized NaPAA¹³ give f independent of C_s for all C_s from about 1 to 1000 mM, is not clear. It may be related to the fact that the sulfated styrene side groups of NaPSS are significantly bulkier than the rather "bald" side groups of these latter polyelectrolytes, and hence the NaPSS must swell to relatively more open configurations (higher L_T') before the as yet unexplained draining condition is reached where f becomes independent of C_s . Supporting this conjecture is the fact that proteoglycans, which are sterically very dense polyelectrolyte structures, behave in the nondraining limit over 1–1000 mM C_s .³⁹

We cannot offer a model at this point which embraces both the suggestion of free draining given by f independent of C_s and the nondraining implication of $f \propto M^{0.5}$ although it seems plausible that electrostatically based polymer expansion should have less effect on impeding solvent flow than the corresponding effects caused by hard excluded volume. For NaPSS, at least, it seems that at high C_s the nondraining limit usually assumed for long, flexible neutral polymers is reached. After the transition to the plateau of f vs C_s there seems to be some type of almost exact cancellation between the effects of added coil expansion increasing f and increased draining lowering f . Theorists concerned with these issues may find these data present an interesting puzzle. In the meantime, caution is advised when using dynamic light scattering as a means of sizing linear polyelectrolytes.

Acknowledgment. Support for this work from National Science Foundation Grant DMB 8803760 is gratefully acknowledged.

References and Notes

- (1) Yamakawa, H.; Fujii, M. *Macromolecules* **1973**, *6*, 407.
- (2) Kirkwood, J. G.; Riseman, J. *J. Chem. Phys.* **1948**, *16*, 565.
- (3) Wang, S.; Douglas, J. F.; Freed, K. F. *J. Chem. Phys.* **1987**, *2*, 1346.
- (4) Adler, R. S.; Freed, K. F. *J. Chem. Phys.* **1980**, *72*, 2032.
- (5) Zimm, B. H. *Macromolecules* **1984**, *17*, 795.
- (6) Kawahara, K.; Norisue, T.; Fujita, H. *J. Chem. Phys.* **1968**, *49*, 4339.
- (7) Douglas, J. F.; Freed, K. F. *Macromolecules* **1985**, *17*, 2354.
- (8) Wang, S.; Douglas, J. F.; Freed, K. F. *Macromolecules* **1985**, *18*, 2464.
- (9) Debye, P. *Phys. Rev.* **1947**, *71*, 486.
- (10) Mulderje, J. J. H.; Jalink, H. L. *Macromolecules* **1987**, *20*, 1152.
- (11) Comper, W. D.; Laurent, T. C. *Physiol. Rev.* **1978**, *58*, 1, 255.
- (12) Ghosh, S.; Li, X.; Reed, C. E.; Reed, W. F. *Biopolymers* **1990**, *30*, 1101.
- (13) Reed, W. F.; Ghosh, S.; Medahdi, G.; François, J. *Macromolecules* **1991**, *24*, 6189.
- (14) Lin, S. C.; Lee, W. I.; Schurr, J. M. *Biopolymers* **1978**, *17*, 1041.
- (15) Ghosh, S.; Peitzsch, R. M.; Reed, W. F., submitted for publication in *Biopolymers*.
- (16) Communication with Larry Rosen at Pressure Chemical Co., 3419-25 Smallman St., Pittsburgh, PA 15201.
- (17) Drifford, M.; Belloni, L.; Dabiez, J. P.; Chattopadhyay, A. K. *J. Colloid Interface Sci.* **1985**, *105*, 2, 587.
- (18) Manning, G. S. *J. Chem. Phys.* **1969**, *51*, 924.
- (19) Förster, S.; Schmidt, M.; Antonietti, M. *Polymer* **1990**, *31*, 781.
- (20) Reed, C. E.; Li, X.; Reed, W. F. *Biopolymers* **1989**, *28*, 1981.
- (21) Odijk, T. *J. Polym. Sci., Polym. Phys. Ed.* **1977**, *15*, 477.
- (22) Skolnick, J.; Fixman, M. *Macromolecules* **1977**, *10*, 944.
- (23) Odijk, T.; Houwaart, A. C. *J. Polym. Sci., Polym. Phys. Ed.* **1978**, *16*, 627.
- (24) Fixman, M.; Skolnick, J. *Macromolecules* **1978**, *11*, 863.
- (25) Reed, C. E.; Reed, W. F. *J. Chem. Phys.* **1990**, *92*, 6916.
- (26) Reed, C. E.; Reed, W. F. *J. Chem. Phys.* **1991**, *94*, 8479.
- (27) Gupta, S. K.; Forsman, W. C. *Macromolecules* **1972**, *5*, 779.
- (28) Forsman, W. C. In *Polymers in Solution*; Forsman, W. C., Ed.; Plenum: New York, 1986.
- (29) Yamakawa, H. *Modern Theory of Polymer Solutions*; Harper and Row: New York, 1971.
- (30) Tanford, C. *Physical Chemistry of Macromolecules*; John Wiley and Sons: New York, 1961.
- (31) Khorramian, B. A.; Stivala, S. S. *Arch. Biochem. Biophys.* **1986**, *2*, 384.
- (32) Loucas, S. P.; Yeh, K. C.; Haddad, H. M. *J. Pharm. Sci.* **1971**, *60*, 7, 1109.
- (33) Miklantz, H.; Riemann, J.; Vidic, H. J. *J. Liq. Chromatogr.* **1986**, *9*, 10, 2073.
- (34) Nakagaki, M.; Sano, Y. *Bull. Chem. Soc. Jpn.* **1972**, *45*, 1011.
- (35) Nakagaki, M.; Ikeda, K. *Bull. Chem. Soc. Jpn.* **1968**, *41*, 555.
- (36) Pasternack, S. G.; Veis, A.; Breen, M. J. *Biol. Chem.* **1974**, *249*, 7, 2206.
- (37) Wasteson, A. *Biochem. J.* **1971**, *122*, 477.
- (38) Tivant, P.; Turq, P.; Drifford, M.; Magdelenat, H.; Menez, R. *Biopolymers* **1983**, *22*, 643.
- (39) Li, X.; Reed, W. F. *J. Chem. Phys.* **1991**, *94*, 4568.
- (40) Davis, R. M.; Russel, W. B. *J. Polym. Sci. B* **1986**, *24*, 511.
- (41) Tricot, M. *Macromolecules* **1984**, *17*, 1698.
- (42) Schmidt, M.; Stockmayer, W. H. *Macromolecules* **1984**, *17*, 509.
- (43) Wang, S.; Douglas, J. F.; Freed, K. F. *J. Chem. Phys.* **1986**, *85*, 3674.
- (44) Freed, K. F.; Wang, S.; Rouvers, J.; Douglas, J. F. *Macromolecules* **1988**, *21*, 2219.
- (45) Koene, R. S.; Smit, H. W. J.; Mandel, M. *Chem. Phys. Lett.* **1980**, *74*, 1, 176.
- (46) Koene, R. S.; Mandel, M. *Macromolecules* **1983**, *16*, 220.
- (47) Koene, R. S.; Nicolai, T.; Mandel, M. *Macromolecules* **1983**, *16*, 227.
- (48) Kowblansky, M.; Zema, P. *Macromolecules* **1982**, *15*, 788.

Registry No. Hep, 9005-49-6; ChS, 25322-46-7; (NaPSS) (homopolymer), 9080-79-9.